

Heart Rate Variability predicts the Subject-Driven Cognitive States

Carlos Enrique Paucar Farfán

Universidade de São Paulo

Grover Enrique Castro Guzman

Universidade de São Paulo

Pedro Briel

Universidade de São Paulo

Alfredo Goldman

Universidade de São Paulo

Daniel Yasumasa Takahashi

Federal University of Rio Grande do Norte

Andre Fujita (✉ andrefujita@usp.br)

Universidade de São Paulo

Article

Keywords:

Posted Date: August 18th, 2022

DOI: <https://doi.org/10.21203/rs.3.rs-1957712/v1>

License:   This work is licensed under a Creative Commons Attribution 4.0 International License.

[Read Full License](#)

Heart Rate Variability predicts the Subject-Driven Cognitive States

Carlos Enrique Paucar Farfán¹, Grover Enrique Castro Guzman¹, Pedro Bruel¹, Alfredo Goldman¹, Daniel Yasumasa Takahashi², and Andre Fujita^{1,*}

¹Department of Computer Science, Institute of Mathematics and Statistics, University of São Paulo, Brazil

²Brain Institute, Federal University of Rio Grande do Norte, Rio Grande do Norte, Brazil

*andrefujita@usp.br

ABSTRACT

Methods for controlling machines using physiological signals have been the focus of much research over the last decades. One natural approach is to use brain signals for decoding subject-driven cognitive states. However, brain-based decoding approaches often require costly, challenging to handle, and uncomfortable devices inadequate for daily use. We propose an alternative method to decode cognitive states based on heart rate (HR). Although HR is capable of classifying general physiological conditions (*e.g.*, level of physical activities, stress, some diseases), it is less clear if HR signals can discriminate cognitive states. To answer this question, we submitted 25 subjects (mean age \pm standard deviation, 30.2 ± 4.9 y.o.) to four cognitive tasks: (i) resting quietly, (ii) remembering their day's events, (iii) singing lyrics, and (iv) subtracting numbers. We collected the electrocardiogram twice for each individual, separated by approximately one week. We used an inexpensive commercially available chest sensor band to collect the HR. We trained a support vector machine to classify the cognitive tasks using data collected on day one. Then we validated it in the dataset collected on day two. Our results show classification accuracy higher than expected at random ($p < 0.001$, bootstrap test). Therefore, we conclude that we can use HR to help decode cognitive states. Because we can easily monitor the HR using a wearable sensor, HR is potentially helpful for human-machine interface applications in daily conditions.

1 Introduction

Brain decodification, *i.e.*, the discrimination of specific cognitive states, has gained much attention over the last decades as a tool for the human-machine interface¹. Many approaches have yielded remarkable results in classification accuracy using functional magnetic resonance imaging (fMRI)², electroencephalography (EEG)³, electrocorticography (ECoG)⁴, or functional near-infrared spectroscopy (fNIRS)⁵. However, brain signal-based methods present some critical limitations⁶. For example, they are costly, present low signal-to-noise ratios, and limit individual mobility for daily use⁷.

In contrast to brain signals, we can measure heart signals using readily and inexpensively available systems, such as smartwatches and chest bands⁸. Moreover, heart rate signals have a larger signal-to-noise ratio than brain signals⁹. Hence they are more robust against body movements. Here, we propose to use heart rate variability (HRV), which measures the variation in time between heartbeats, for decoding cognitive state. The rationale for using the HRV is that it is strongly associated with autonomic nervous system (ANS) activity. The ANS regulates not only our heart rate, blood pressure, breathing, and digestion but also modulates the interoceptive processes, *i.e.*, the sense of the body's internal state¹⁰.

Given that several interoception-related brain areas are critical for cognitive processes, it is natural to ask whether interoceptive processes modulate cognition¹¹. Despite this theoretical possibility, studies using HR - a proxy of ANS activity - have focused only on emotional and metabolic aspects of behavior. The possibility that HR may be associated with the cognitive process is mainly unexplored¹². We hypothesize that HR is a good proxy for the brain's cognitive states. In particular, we expect to be able to discriminate cognitive states using HR.

2 Materials and Methods

We want to test the hypothesis that the cardiac signal has information about the subject-driven cognitive state. To test this hypothesis, we recruited 30 subjects (section 2.1), used a subject-driven cognitive states experiment (section 2.2), collected (section 2.3), pre-processed (section 2.4), and extracted metrics from the HR (section 2.5), and finally used a machine learning classifier to discriminate the cognitive states (section 2.6).

2.1 Subjects

Thirty healthy right-handed subjects (all males) aged 23–44 participated in this study. Eligible subjects were healthy and right-handed males (to avoid dominant hand bias and gender effect) between 20 and 45 years old. Exclusion criteria were: the presence of cardiorespiratory disease, use of drugs/medicine, ingestion of caffeine or alcohol, exhaustive exercises 24 hours before data collection, and do not sleep well at least seven hours the night before data collection.

We excluded five subjects due to auto declaration of discomfort, nervousness, or caffeine consumption. Thus, our final dataset comprised 25 subjects (mean age \pm standard deviation, 30.2 ± 4.9 y.o.). This number of subjects is similar to the one described in¹³, the work we based our experimental design. Besides cardiac signal acquisition (please refer to section 2.4 for further details), we also collected height, weight, frequencies of coffee consumption, and physical activity.

The Ethics Committee for Human Research at the Escola de Artes, Ciências e Humanidades (EACH) - the University of São Paulo (USP) approved the experimental protocol (protocol number: 32732320.4.0000.5390; date of approval: June 9th, 2020). All experiments were performed in accordance with the ethics committee guidelines and regulations. Informed consent was obtained from all participants.

2.2 Experimental design

The experimental design was the same as carried out by¹³ in neuroscience. They designed these experiments to make the cognitive states similar to reality.

We instructed the subjects to sit upright and close their eyes. All subjects completed four 10-min tasks described in¹³: (1) a resting-state electrocardiogram, (2) an episodic memory task, (3) a music lyrics task, and (4) a subtraction task. Subjects always completed the resting-state electrocardiogram first, and we balanced the order of the three cognitive tasks. Details of each task are as follows:

1. *Resting state.* We instructed subjects to relax, let their minds wander, and try not to focus on anything.
2. *Memory task.* We asked subjects to recall the day's events from when they awoke until the moment of the experiment.
3. *Music task.* We asked subjects to sing their favorite songs mentally.
4. *Subtraction task.* We asked subjects to count backward from some randomly chosen number greater than 5 000 by 7s.

We recruited the subjects twice, separated by approximately one week. In other words, each subject performed the four tasks twice. We collected all the data before noon. We carried out most of the second-week data collection approximately at the same time as the first collection.

2.3 Cardiac signal acquisition

We used the Polar H10 chest strap sensor (<https://www.polar.com/br>) to monitor the cardiac signal. Studies carried out in controlled environments with the electrocardiogram (ECG), the gold standard, showed that this type of sensor presents sampling rates and precision sufficient to capture HR^{7,14}. Also, Polar sensors present a high correlation to ECG¹⁵.

The Polar H10 sensor collects an electrocardiogram at a frequency of 1kHz. It transmits the RR interval (the time elapsed between two successive R spikes in the QRS complex of the electrocardiogram wave) data through Bluetooth low energy at a frequency of 1Hz. For continuous data collection, we developed a Python software. This software stores the data in a document-based database.

2.4 Cardiac signal preprocessing

Although the heart's positioning guarantees a clean signal, the ECG is not free of noise and artifacts. One natural cause is ectopic beats, caused by electric conductivity originating in the fibers outside the sinoatrial node. The sinoatrial node is the cardiac muscle region responsible for electric impulses. Other causes are the sensor's lack of contact with the skin or lousy detection of the QRS complex peaks. Thus, we preprocessed the data using the gHRV software¹⁶. The preprocessing steps were as follows:

1. We excluded the outliers, it i.e., RR intervals lower than 300ms and greater than 2 000ms.
2. We filtered out ectopic beats in short-term HR using the technique described by¹⁷. We followed the suggestions of¹⁸ and applied a 4Hz interpolation to complete the missing points.
3. We calculated the RR normalized intervals (NN).

Because our Python software collected the data at a frequency of 1Hz and each individual carried out each task for approximately 10 minutes, each cardiac signal time series comprised approximately 600-time points. We excluded the first 50 seconds of each task to guarantee that we considered data when the subjects were focused on the task. We constructed sliding windows of 45 seconds for feature extraction, with a second displacement to calculate the next immediate sliding window. Thus, we represented each individual with approximately 500 sliding windows.

2.5 Cardiac signal metrics

We calculated the most commonly used HRV metrics¹⁹ for each sliding window as follows. We describe between parenthesis the unit of measurement.

1. Mean of heart rates (beats per minute - bpm):

$$\text{MHR} = \frac{1}{n} \sum_{i=1}^n \text{HR}_i \quad (1)$$

2. Mean of RR intervals (milliseconds - ms):

$$\text{MRR} = \frac{1}{n} \sum_{i=1}^n \text{RR}_i \quad (2)$$

3. Root mean square of successive RR interval differences (ms):

$$\text{rMSSD} = \sqrt{\frac{1}{n} \sum_{i=1}^{n-1} (\text{RR}_{i+1} - \text{RR}_i)^2} \quad (3)$$

4. Heart rate standard deviation (bpm):

$$\text{HRSTD} = \sqrt{\frac{1}{n-1} \sum_{i=1}^{n-1} (\text{HR}_i - \text{MHR})^2} \quad (4)$$

5. Standard deviation of the normalized RR (NN) (ms):

$$\text{SDNN} = \sqrt{\frac{1}{n-1} \sum_{i=1}^n (\text{NN}_i - \text{MRR})^2} \quad (5)$$

6. Coefficient of variation of normalized RR intervals:

$$\text{CV_RR} = \text{SDNN}/\text{MRR} \quad (6)$$

7. Percentage of successive normalized RR intervals that differ by more than 50 ms (%):

$$\text{pNN50} = \frac{\#(\text{NN} > 50)}{\#(\text{NN})} \quad (7)$$

8. Power of the low-frequency (LF) band (0.04–0.15Hz) (ms^2).

9. Power of the high-frequency (HF) band (0.15–0.4Hz) (ms^2).

10. Ratio of LF-to-HF power (LFHF) (%).

11. The approximate entropy (ApEn) measures the regularity and complexity of a time series²⁰. Let $C_m(r)$ be the prevalence of repetitive patterns of length m , and r be the similarity criterion; then, the approximate entropy is defined as follows:

$$\text{ApEn} = \ln \left[\frac{C_m(r)}{C_{m+1}(r)} \right] \quad (8)$$

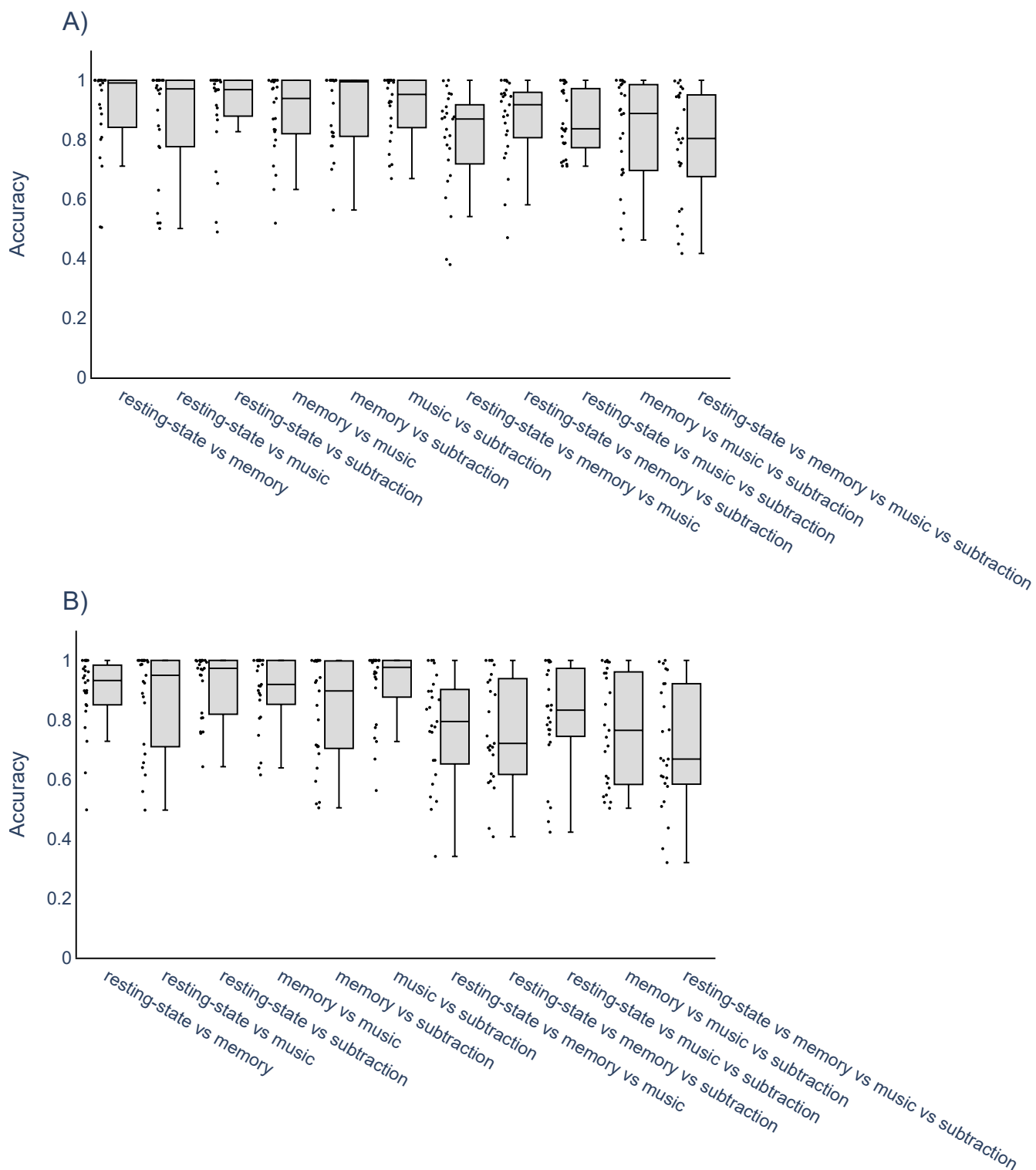


Figure 1. Within-day subject-driven cognitive states classification accuracies. (A) We obtained the classification accuracies using the first half of day one data as the training dataset and the second half as the validation set. (B) We obtained the classification accuracies using the first half of day two data as the training set and the second half as the validation set.

12. The fractal dimension (FracDim) measures the complexity of the HRV signal. It quantifies the time series self-similarity characteristics. We performed the calculations according to the algorithm described in²¹. Let C_m be the prevalence of repetitive patterns of length m , and r_a and r_b be two different similarity criteria. Then, the fractal dimension is defined as follows:

$$\text{FracDim} = \frac{\ln(C_m(r_b)) - \ln(C_m(r_a))}{\ln(r_b) - \ln(r_a)} \quad (9)$$

We did not calculate the ULF (≤ 0.003 Hz) and VLF (0.0033 – 0.04 Hz) bands because they are only helpful for data measured using 24 hours recordings.

2.6 Data classification

We used the support vector machine (SVM) with radial basis functions kernel as suggested by²² for ECG classification.

SVMs are supervised learning methods for classification analysis. Suppose we have a training set, *i.e.*, a set of cardiac signals, each labeled as belonging to one of the four groups (resting-state, memory, music, subtraction). Then, an SVM training algorithm builds a model that assigns new cardiac signals to one of the groups. SVM maps training cardiac signals to points in space to maximize the width of the gap between the groups. For new cardiac signals, SVM maps them into that same space and predicts to which group the new (unlabeled) cardiac signal belongs based on which side of the gap they fall.

SVMs can efficiently perform linear and nonlinear classifications. SVM uses the kernel trick for nonlinear classification, mapping the inputs into high-dimensional feature spaces. Here we used the nonlinear classification suggested by²² for cardiac signal classification.

To evaluate the classification accuracy, we performed two experiments. One was to test whether we could discriminate the subject's physiological condition within the day. To this end, we split the data into two parts for each individual: the first half of the time series as the training dataset and the second half as the validation dataset. The other was to test whether we could discriminate the subject's physiological condition between days. To this end, we used the dataset collected on day one as the training dataset and the dataset collected on day two as the validation dataset.

To compare our results to the ones obtained by¹³, we used the same leave-one-out cross-validation (LOOCV). LOOCV consists of using one observation as the validation set and the remaining observations as the training set. We repeat it for all observations.

We used D-optimal Design²³, a Julia library²⁴, to identify the most critical features described in section 2.5 for task classification. We converted the importance to percentages for better interpretation.

2.7 Statistical analysis

We used Spearman's correlation to test the association between the cognitive state classification accuracy and clinical variables, such as height, weight, and frequency of physical activity. Spearman's correlation is a nonparametric method to test the statistical dependence between the rankings of two variables. It assesses how well we can describe the relationship between two variables using a monotonic function²⁵. We assumed a p-value cutoff of 0.05 for statistical significance in a bootstrap test.

3 Results

Figure 1 shows the classification accuracies for all classification combinations using the first (panel A) and second days (panel B). As expected, the classification accuracies decreased as the number of considered cognitive states increased in both cases. The average classification accuracy was more significant for all of them than we expected at random ($p < 0.001$, bootstrap test). In other words, for two, three, and four class comparisons, we obtained average accuracies more significant than 50, 33, and 25%. The classification accuracies obtained within the first and second days were similar.

The second experiment tested whether we could discriminate against the subject's physiological condition between days. To this end, for each individual, we used the data collected on the first day as the training set and the data collected on the second day as the validation dataset. Figure 2 shows the classification accuracies for the 25 participants in each classification combination. As expected, the classification accuracies decreased as the number of considered cognitive states increased. Again, the average accuracy was significantly greater for all between-day classifications than we expected at random ($p < 0.001$, bootstrap test). However, here, the accuracies were smaller than the within-day equivalent comparison. Thus, it seems that the cardiac signal was day-dependent. In other words, we had an information loss between days. One intuitive normalization factor in improving the classification accuracy could be the resting state cardiac signal. Thus, we included it as a covariate, but the accuracy did not increase.

To compare our results to the ones obtained by¹³ using the fMRI, we performed the leave-one-out cross-validation (LOOCV) analysis for the four-classes classification. We achieved an average accuracy of approximately 46% in this analysis ($p < 0.001$, bootstrap test).

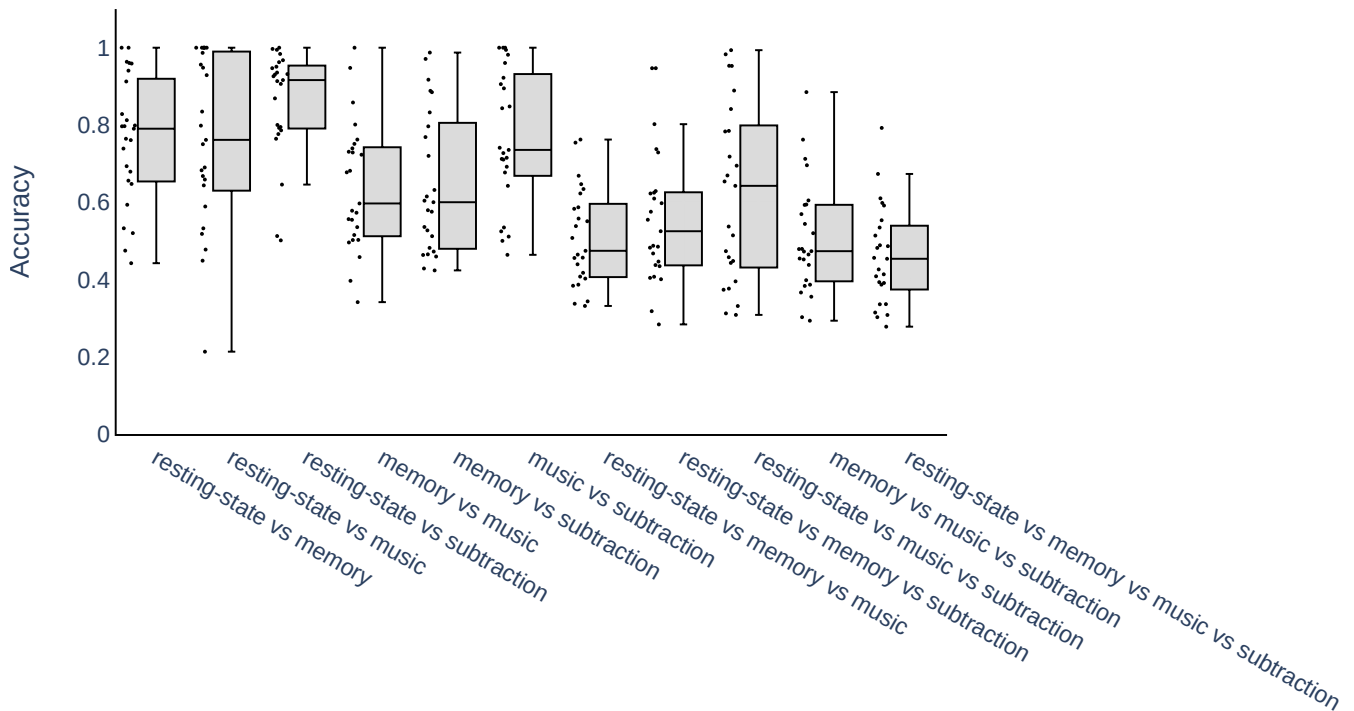


Figure 2. Between-day subject-driven cognitive states classification accuracies. We used the day one data as the training set and day two as the validation set.

We also asked if the individual physical differences were relevant for classification performance. Hence, we tested whether classification accuracy correlates to other participants' height, weight, and physical activity practice. None were statistically significant ($p > 0.05$, bootstrap test), showing that physical differences between individuals were not predictive of the accuracy of the classifier.

Among all the features we used for classification, it is natural to ask which features are the most relevant ones. Figure 3 shows the importance of each feature for task classification. We can see that HR and NN intervals are the first and second most critical task classification characteristics.

4 Discussion

We presented the HR-based cognitive state classification results obtained in two conditions: within and between days. For both within and between-day experiments, the accuracy was more significant than we expected at random. This result is consistent with the hypothesis that HR can be used to encode cognitive states. We also analyzed which HR-based features were essential for the classification. The two most important are the raw HR and NN (RR normalized intervals), which correspond to approximately 40% of the features.

We used four self-driven cognitive tasks previously used in an fMRI study to decode cognitive states: (i) resting, (ii) memory, (iii) music, and (iv) subtraction¹³. This experimental design presented at least two main challenges. First, we acquired the HR in continuous runs with no stimulus presentation and no investigator-imposed temporal landmarks other than the scan's start and end of the session. Hence, there was no apparent onset or offset for events. This is an experimental design that better mimics a more realistic situation than event-based brain decoding experiments^{26–35}. Second, we based the decoding on a single HR signal, which presents a much smaller degree of freedom than high-dimensional brain signals. To compare our classifier based on the HR to what we would expect by using an fMRI-based approach, we carried out a LOOCV experiment similar to the one presented in¹³. In the LOOCV experiment for four classes classification, we obtained an average accuracy of 46%, significantly lower than the 85% obtained by¹³. This result is expected, given that we used only one signal. In contrast,¹³ used 90 regions of interest (ROI) of the brain.

One may ask why we could distinguish the four cognitive tasks using only the cardiac signal. One possible explanation is that the HRV measures interoception, *i.e.*, the perception of the body's physiological conditions^{36,37}. HRV represents compressed information about how the body interacts with the brain. Also, as aforementioned, the brain and heart are connected by the autonomic nervous system. HRV represents the organism's internal state. It is considered an indicator of the autonomic

	resting-state vs memory	resting-state vs music	resting-state vs subtraction	memory vs music	memory vs subtraction	music vs subtraction	resting-state vs memory vs music	resting-state vs memory vs subtraction	resting-stage vs music vs subtraction	memory vs music vs subtraction	resting-stage vs memory vs music vs subtraction
NN	10.68%	7.87%	13.65%	17.18%	13.29%	13.60%	14.21%	13.30%	13.04%	10.85%	11.96%
HR	32.37%	19.20%	29.67%	15.11%	20.46%	26.66%	27.32%	28.90%	28.99%	18.38%	27.17%
MHR	6.15%	17.66%	6.52%	0.52%	6.75%	4.27%	7.92%	9.54%	8.99%	7.35%	7.88%
MRR	7.12%	12.67%	8.01%	0.86%	1.84%	2.39%	4.10%	5.20%	4.93%	6.07%	6.79%
rMSSD	0.32%	7.67%	0.00%	0.00%	0.00%	0.00%	0.54%	0.00%	1.74%	0.00%	0.00%
HRSTD	6.80%	8.25%	7.13%	6.53%	7.37%	9.60%	9.02%	7.22%	7.53%	8.46%	8.97%
SDNN	4.53%	9.79%	5.34%	1.38%	4.29%	2.14%	1.91%	2.89%	3.19%	5.34%	4.08%
CV_RR	0.00%	0.58%	2.67%	6.53%	6.14%	3.20%	0.00%	3.18%	2.32%	2.94%	2.18%
pNN50	9.06%	0.20%	6.23%	12.37%	6.54%	5.86%	8.19%	7.22%	4.34%	5.69%	4.61%
LF	6.80%	4.99%	5.34%	8.77%	8.59%	8.80%	7.38%	6.36%	7.83%	9.01%	8.15%
HF	2.91%	4.80%	2.97%	7.73%	5.52%	6.39%	3.55%	2.89%	5.21%	7.54%	5.43%
LFHF	0.32%	0.00%	0.00%	7.39%	4.29%	3.20%	5.19%	0.57%	0.00%	2.57%	0.00%
ApEn	7.12%	0.38%	7.42%	12.54%	12.27%	9.60%	7.65%	8.96%	7.53%	10.85%	8.69%
FracDim	5.82%	5.95%	5.05%	3.10%	2.66%	4.27%	3.01%	3.76%	4.34%	4.97%	4.08%

Figure 3. Features importance in between-day analyses. The darker the cell is, the more critical the respective feature. The number in each cell describes the importance of the feature in percentage.

nervous system, *i.e.*, a global parameter representing the body’s behavioral state ^{14,38}.

Although the brain-scanning based classifier had better performance than our proposal, they present some critical disadvantages. For example, we need specialized knowledge for equipment set up and powerful computational resources for data processing. Besides, they are costly and present low signal-to-noise ratios. Furthermore, mobility is very limited or impossible, making their use in our daily lives prohibitive⁷. In our experiments, instead of using an ECG usually present in hospitals, we used a wearable sensor (Polar H10 chest strap), focusing on the future daily use of the HRV. Our proposal is noninvasive, inexpensive, and with a simple setup. Also, HRV collected using the Polar H10 sensor presents a high correlation to electrocardiography (ECG), which is considered the gold standard for HRV measurement. Finally, ECG presents orders of magnitude higher signal-to-noise ratio than brain-scanning technologies because the heart’s electrical signal is large. Therefore, HRV is a viable alternative solution for cognitive decoding.

Our raw data for this work is available on the following website:

https://github.com/caiki/HRV_DB_CognitiveStates.

We believe this dataset may be helpful for AI researchers looking for well-controlled benchmarks to evaluate their computational approaches.

5 Conclusions

Here we provided evidence that the HRV contains information regarding cognitive states. Also, results in subjective-driven tasks suggest its usefulness in situations closer to daily conditions. Altogether, HRV can be an alternative for brain-based cognitive states classification for daily life use.

Competing Interests Statement

The authors declare that the research was conducted in the absence of any commercial or financial relationships that could be construed as a potential conflict of interest.

Author Contributions

C.E.P.F., G.E.C.G, and P.B. implemented the classification and performed the experiments and analyses. C.E.P.F. collected the clinical and HRV samples. A.G. supervised the features importance analysis. D.Y.T. and AF designed the study. A.F. led the study. All authors read and approved the final version of the manuscript.

Acknowledgements

This work was supported by the FAPESP (2018/21934-5 and 2020/01479-1), CNPq (303855/2019-3), CAPES (Finance code 001), Alexander von Humboldt Foundation, the Academy of Medical Sciences-Newton Fund, Wellcome Leap, and the Hewlett Packard Enterprise.

Data Availability Statement

The HRV datasets for this study can be found in the GitHub https://github.com/caiki/HRV_DB_CognitiveStates.

References

1. Gao, X., Wang, Y., Chen, X. & Gao, S. Interface, interaction, and intelligence in generalized brain–computer interfaces. *Trends cognitive sciences* **25**, 671–684, DOI: [10.1016/j.tics.2021.04.003](https://doi.org/10.1016/j.tics.2021.04.003) (2021).
2. Sorger, B. & Goebel, R. Real-time fmri for brain-computer interfacing. *Handb. clinical neurology* **168**, 289–302, DOI: [10.1016/B978-0-444-63934-9.00021-4](https://doi.org/10.1016/B978-0-444-63934-9.00021-4) (2020).
3. Schirrmester, R. T. *et al.* Deep learning with convolutional neural networks for EEG decoding and visualization. *Hum. Brain Mapp.* **38**, 5391–5420, DOI: [10.1002/hbm.23730](https://doi.org/10.1002/hbm.23730) (2017).
4. Shiraishi, Y. *et al.* Neural decoding of electrocorticographic signals using dynamic mode decomposition. *J. Neural Eng.* **17**, 036009, DOI: [10.1088/1741-2552/ab8910](https://doi.org/10.1088/1741-2552/ab8910) (2020).
5. Hong, K. S., Khan, M. J. & Hong, M. J. Feature Extraction and Classification Methods for Hybrid fNIRS-EEG Brain-Computer Interfaces, DOI: [10.3389/fnhum.2018.00246](https://doi.org/10.3389/fnhum.2018.00246) (2018).
6. Lee, D.-H., Jeong, J.-H., Kim, K., Yu, B.-W. & Lee, S.-W. Continuous eeg decoding of pilots' mental states using multiple feature block-based convolutional neural network. *IEEE access* **8**, 121929–121941, DOI: [10.1109/ACCESS.2020.3006907](https://doi.org/10.1109/ACCESS.2020.3006907) (2020).
7. Zehr, E. P. Future think: Cautiously optimistic about brain augmentation using tissue engineering and machine interface. *Front. Syst. Neurosci.* **9**, 1–5, DOI: [10.3389/fnsys.2015.00072](https://doi.org/10.3389/fnsys.2015.00072) (2015).
8. Kunkels, Y. K., van Roon, A. M., Wichers, M. & Riese, H. Cross-instrument feasibility, validity, and reproducibility of wireless heart rate monitors: Novel opportunities for extended daily life monitoring. *Psychophysiology* **58**, e13898, DOI: [10.1111/psyp.13898](https://doi.org/10.1111/psyp.13898) (2021).
9. Lee, D., Kwon, W., Heo, J. & Park, J. Y. Associations between heart rate variability and brain activity during a working memory task: A preliminary electroencephalogram study on depression and anxiety disorder. *Brain sciences* **12**, 172, DOI: [10.3390/brainsci12020172](https://doi.org/10.3390/brainsci12020172) (2022).
10. Berntson, G. G., Gianaros, P. J. & Tsakiris, M. Interoception and the autonomic nervous system: Bottom-up meets top-down. *The interoceptive mind. From homeostasis to awareness* 3–23, DOI: [10.1093/oso/9780198811930.001.0001](https://doi.org/10.1093/oso/9780198811930.001.0001) (2018).
11. Berntson, G. G. & Khalsa, S. S. Neural circuits of interoception. *Trends neurosciences* **44**, 17–28 (2021).
12. Alaiti, R. K. *Movement-related pain as a learned response: an investigation of the possible mechanisms underlying movement-related pain persistence and recovery in subjects with chronic musculoskeletal pain*. Ph.D. thesis, Universidade de São Paulo (2021).
13. Shirer, W. R., Ryali, S., Rykhlevskaia, E., Menon, V. & Greicius, M. D. Decoding subject-driven cognitive states with whole-brain connectivity patterns. *Cereb. Cortex* **22**, 158–165, DOI: [10.1093/cercor/bhr099](https://doi.org/10.1093/cercor/bhr099) (2012).

14. Julien, C. The enigma of Mayer waves: Facts and models, DOI: [10.1016/j.cardiores.2005.11.008](https://doi.org/10.1016/j.cardiores.2005.11.008) (2006).
15. Plews, D. J. *et al.* Comparison of Heart-Rate-Variability Recording With Smartphone Photoplethysmography, Polar H7 Chest Strap, and Electrocardiography. *Int. J. Sports Physiol. Perform.* **12**, 1324–1328, DOI: [10.1123/ijsp.2016-0668](https://doi.org/10.1123/ijsp.2016-0668) (2017).
16. Rodríguez-Liñares, L., Lado, M., Vila, X., Méndez, A. & Cuesta, P. gHRV: Heart rate variability analysis made easy. *Comput. Methods Programs Biomed.* **116**, 26–38, DOI: [10.1016/J.CMPB.2014.04.007](https://doi.org/10.1016/J.CMPB.2014.04.007) (2014).
17. Acar, B., Savelieva, I., Hemingway, H. & Malik, M. Automatic ectopic beat elimination in short-term heart rate variability measurement. *Comput. Methods Programs Biomed.* **63**, 123–131, DOI: [10.1016/S0169-2607\(00\)00081-X](https://doi.org/10.1016/S0169-2607(00)00081-X) (2000).
18. Singh, D., Vinod, K. & Saxena, S. C. Sampling frequency of the RR interval time series for spectral analysis of heart rate variability. *J. Med. Eng. Technol.* **28**, 263–272, DOI: [10.1080/03091900410001662350](https://doi.org/10.1080/03091900410001662350) (2004).
19. Shaffer, F. & Ginsberg, J. P. An overview of heart rate variability metrics and norms. *Front. public health* **258** (2017).
20. Pham, T., Lau, Z. J., Chen, S. H. A. & Makowski, D. Heart rate variability in psychology: A review of hrv indices and an analysis tutorial. *Sensors* **21**, DOI: [10.3390/s21123998](https://doi.org/10.3390/s21123998) (2021).
21. Kaplan, D. T., Furman, M. I. & Pincus, S. M. Techniques for analyzing complexity in heart rate and beat-to-beat blood pressure signals. In *Computers in Cardiology*, 243–246, DOI: [10.1109/cic.1990.144206](https://doi.org/10.1109/cic.1990.144206) (Publ by IEEE, 1991).
22. Park, D., Lee, M., Park, S., Seong, J.-K. & Youn, I. Determination of Optimal Heart Rate Variability Features Based on SVM-Recursive Feature Elimination for Cumulative Stress Monitoring Using ECG Sensor. *Sensors* **18**, 2387, DOI: [10.3390/s18072387](https://doi.org/10.3390/s18072387) (2018).
23. Jones, B., Allen-Moyer, K. & Goos, P. A-optimal versus d-optimal design of screening experiments. *J. Qual. Technol.* **53**, 369–382, DOI: [10.1080/00224065.2020.1757391](https://doi.org/10.1080/00224065.2020.1757391) (2021).
24. Pedro Buel. [phrb/experimentaldesign.jl](https://zenodo.org/record/4660441), DOI: [10.5281/zenodo.4660441](https://doi.org/10.5281/zenodo.4660441) (2021).
25. de Siqueira Santos, S., Takahashi, D. Y., Nakata, A. & Fujita, A. A comparative study of statistical methods used to identify dependencies between gene expression signals. *Briefings bioinformatics* **15**, 906–918 (2014).
26. Biswal, B., Zerrin Yetkin, F., Haughton, V. M. & Hyde, J. S. Functional connectivity in the motor cortex of resting human brain using echo-planar mri. *Magn. Reson. Medicine* **34**, 537–541, DOI: [10.1002/mrm.1910340409](https://doi.org/10.1002/mrm.1910340409) (1995).
27. Hampson, M., Peterson, B. S., Skudlarski, P., Gatenby, J. C. & Gore, J. C. Detection of functional connectivity using temporal correlations in MR images. *Hum. Brain Mapp.* **15**, 247–262, DOI: [10.1002/hbm.10022](https://doi.org/10.1002/hbm.10022) (2002).
28. Greicius, M. D., Krasnow, B., Reiss, A. L. & Menon, V. Functional connectivity in the resting brain: A network analysis of the default mode hypothesis. *Proc. Natl. Acad. Sci. United States Am.* **100**, 253–258, DOI: [10.1073/pnas.0135058100](https://doi.org/10.1073/pnas.0135058100) (2003).
29. Kiviniemi, V., Kantola, J. H., Jauhiainen, J., Hyvärinen, A. & Tervonen, O. Independent component analysis of nondeterministic fMRI signal sources. *NeuroImage* **19**, 253–260, DOI: [10.1016/S1053-8119\(03\)00097-1](https://doi.org/10.1016/S1053-8119(03)00097-1) (2003).
30. Beckmann, C. F., DeLuca, M., Devlin, J. T. & Smith, S. M. Investigations into resting-state connectivity using independent component analysis. *Philos. Transactions Royal Soc. B: Biol. Sci.* **360**, 1001–1013, DOI: [10.1098/rstb.2005.1634](https://doi.org/10.1098/rstb.2005.1634) (2005).
31. Bellec, P. *et al.* Identification of large-scale networks in the brain using fMRI. *NeuroImage* **29**, 1231–1243, DOI: [10.1016/j.neuroimage.2005.08.044](https://doi.org/10.1016/j.neuroimage.2005.08.044) (2006).
32. Damoiseaux, J. S. *et al.* Consistent resting-state networks across healthy subjects. *Proc. Natl. Acad. Sci. United States Am.* **103**, 13848–13853, DOI: [10.1073/pnas.0601417103](https://doi.org/10.1073/pnas.0601417103) (2006).
33. Seeley, W. W. *et al.* Dissociable intrinsic connectivity networks for salience processing and executive control. *J. Neurosci.* **27**, 2349–2356, DOI: [10.1523/JNEUROSCI.5587-06.2007](https://doi.org/10.1523/JNEUROSCI.5587-06.2007) (2007).
34. Kiviniemi, V. *et al.* Functional segmentation of the brain cortex using high model order group PICA. *Hum. Brain Mapp.* **30**, 3865–3886, DOI: [10.1002/hbm.20813](https://doi.org/10.1002/hbm.20813) (2009).
35. Smith, G. E. *et al.* A Cognitive Training Program Based on Principles of Brain Plasticity: Results from the Improvement in Memory with Plasticity-based Adaptive Cognitive Training (IMPACT) Study. *J. Am. Geriatr. Soc.* **57**, 594–603, DOI: [10.1111/j.1532-5415.2008.02167.x](https://doi.org/10.1111/j.1532-5415.2008.02167.x) (2009).
36. Park, H. D. & Tallon-Baudry, C. The neural subjective frame: From bodily signals to perceptual consciousness. *Philos. Transactions Royal Soc. B: Biol. Sci.* **369**, DOI: [10.1098/rstb.2013.0208](https://doi.org/10.1098/rstb.2013.0208) (2014).

37. Craig, A. D. Interoception: The sense of the physiological condition of the body, DOI: [10.1016/S0959-4388\(03\)00090-4](https://doi.org/10.1016/S0959-4388(03)00090-4) (2003).
38. Forte, G., Favieri, F. & Casagrande, M. Heart Rate Variability and Cognitive Function: A Systematic Review. *Front. Neurosci.* **13**, 710, DOI: [10.3389/fnins.2019.00710](https://doi.org/10.3389/fnins.2019.00710) (2019).

Figure legends

Figure 1. Within-day subject-driven cognitive states classification accuracies. (A) We obtained the classification accuracies using the first half of day one data as the training dataset and the second half as the validation set. (B) We obtained the classification accuracies using the first half of day two data as the training set and the second half as the validation set.

Figure 2. Between-day subject-driven cognitive states classification accuracies. We used the day one data as the training set and day two as the validation set.

Figure 3. Features importance in between-day analyses. The darker the cell is, the more critical the respective feature. The number in each cell describes the importance of the feature in percentage.